

Open Access Full Text Article



Research Article

In silico Target Class Prediction and Probabilities for Plant Derived Omega 3 Fatty Acid from Ethyl Acetate Fraction of *Moringa oleifera* Leaf Extract

Murugan M.¹, Krishnaveni K.², Sabitha M.¹, Kandeepan C.¹, Senthilkumar N.³, Loganathan T.⁴, Grace Lydial Pushpalatha G.⁵, Pandiarajan G.⁶, Ramya S.⁷, Jayakumararaj R.^{8*}

¹ PG & Research Department of Zoology, Arulmigu Palaniandavar College of Arts & Culture, Palani – 624601, Dindigul District, TN, India

² Department of Zoology, GTN Arts & Science College, Dindigul - 624005, TN, India

³ Institute of Forest Genetics & Tree Breeding (IFGTB), Indian Council of Forestry Research & Education (ICFRE), Coimbatore – 641002, TN, India

⁴ Department of Plant Biology & Plant Biotechnology, LN Government College (A), Ponneri - 601204, TN, India

⁵ PG Department of Botany, Sri Meenakshi Government Arts College, Madurai-625002, TN, India

⁶ Department of Botany, Sri S Ramasamy Naidu Memorial College (A), Sattur - 626203 TN, India

⁷ PG Department of Zoology, Yadava College (Men), Thiruppalai - 625014, Madurai, TN, India

⁸ PG Department of Botany, Government Arts College, Melur – 625106, Madurai District, TN, India

Article Info:



Article History:

Received 18 April 2022
Reviewed 07 May 2022
Accepted 13 May 2022
Published 20 May 2022

Cite this article as:

Murugan M, Krishnaveni K, Sabitha M, Kandeepan C, Senthilkumar N, Loganathan T, Grace Lydial Pushpalatha G, Pandiarajan G, Ramya S, Jayakumararaj R. In silico Target Class Prediction and Probabilities for Plant Derived Omega 3 Fatty Acid from Ethyl Acetate Fraction of *Moringa oleifera* Leaf Extract. Journal of Drug Delivery and Therapeutics. 2022; 12(3):124-137

DOI: <http://dx.doi.org/10.22270/jddt.v12i3.5352>

*Address for Correspondence:

Jayakumararaj R, PG Department of Botany, Government Arts College, Melur – 625106, Madurai District, TN, India

Abstract

Plant Derived Omega 3 Fatty Acid – α Linolenic Acid (ALA) a carboxylic acid with 18 carbon atoms, 3 cis double bonds. ALA obtained from plant based food source is converted into eicosapentaenoic acid (EPA) and docosahexaenoic acid (DHA). However, the rate of conversion is influenced by dose, gender, and health status. Further, intake of ALA significantly reduces the risk of sudden death among myocardial infarction patients consistent with induced antiarrhythmic effect. ALA is concomitant with cardiovascular-protective, anti-cancer, neuro-protective, anti-osteoporotic, anti-inflammatory, and anti-oxidative properties. ALA has anti-metabolic syndrome that regulates gut-micro-floral functionalities. Clinical trials indicate that ALA can be used in the management of multi-metabolic syndrome effects but in-depth target based ADMET studies are required to ascertain its clinical efficacy and market potential.

Keywords: ADMET; *Moringa oleifera*; Secondary Metabolites; Natural Products (NPs); Bioactive Substances; Octadecatrienoic acid (ODA); Eicosapentaenoic Acid (EPA); Docosahexaenoic Acid (DHA); Plant Derived Omega 3 Fatty Acid (PDO3FA)

INTRODUCTION

Plant Derived Omega 3 Fatty Acid - ALA is considered as an essential fatty acid because it is required for human health, but cannot be synthesized by humans. It is a type of natural fatty acid, commonly known as octadecatrienoic acids¹. Humans can synthesize omega-3 fatty acids from ALA, which includes eicosapentaenoic acid (EPA) and docosahexaenoic acid (DHA). EPA is a precursor of the series-3 prostaglandins, the series-5 leukotrienes and the series-3 thromboxanes². Dietary omega-3 long chain polyunsaturated fatty acids (n-3 LC-PUFA) like eicosapentaenoic acid (EPA, 20:5n-3) and docosahexaenoic acid (DHA, 22:6n-3) are potent metabolic regulators with therapeutic and preventive effects³. These eicosanoids have anti-inflammatory and anti-atherogenic properties⁴. However, it must be pointed out that EPA and DHA are more potent than ALA and SDA (Stearidonic acid) in reducing the risk of

cardiovascular diseases⁵, metabolic inflammation⁶, cancer⁷ and nervous system (CNS) disorders⁸. ALA has been reported to inhibit the production of pro-inflammatory eicosanoids, prostaglandin E2 (PGE2)⁹ and leukotriene B4 (a pro-inflammatory lipid mediator and potent chemo-attractant acting via two G protein-coupled receptors (GPCRs))¹⁰, as well as pro-inflammatory cytokines, tumor necrosis factor-alpha (TNF-alpha) and interleukin-1 beta (IL-1 beta)¹¹.

PDO3FA like ALA and its by-products can modulate the expression of several genes, including those involved in fatty acid metabolism and inflammation^{12,13}. They regulate gene expression by affecting transcription factors including NF-kappa B and members of peroxisome proliferator-activated receptor (PPAR) family^{14,15} or through inhibition of NLRP3 inflammasome activation^{16,17}. Incorporation of ALA and its metabolites in cell membranes can affect membrane fluidity¹⁸.

ALA provide protection against lipopolysaccharide-induced acute lung injury through anti-inflammatory and anti-oxidative pathways¹⁹ besides inhibition of platelet aggregation and possibly in anti-proliferative actions of ALA by delta6 desaturase²⁰.

ALA is a long chain polyunsaturated fatty acid (LC-PUFA) precursor to longer n-6 fatty acids commonly known as omega-6 fatty acids²¹. Omega-6 fatty acids are characterized by a carbon-carbon double bond at the sixth carbon from the methyl group²². Similarly, PUFA alpha-linoleic acid (ALA) is the precursor to n-3 fatty acids known as PDO3FA is characterized by a carbon-carbon double bond at the 3rd carbon from the methyl group²³. ALA undergoes a series of conversions to reach their final fatty acid form²⁴. ALA enters the cell and is catalyzed to gamma-linolenic acid (GLA) by acyl-CoA 6-desaturase (delta-6-desaturase/fatty acid desaturase 2). GLA is then converted to dihomogammalinolenic acid (DGLA) by elongation of very long chain fatty acids protein 5 (ELOVL5). DGLA is then converted to arachidonic acid (AA) by acyl-CoA (8-3)-desaturase (delta-5-desaturase/fatty acid desaturase). Arachidonic acid is then converted to a series of short lived metabolites called eicosanoids before reaching its final form^{25,26}.

ALA chemically (18:3n-3 or 3n-6) is a carboxylic acid with 18 carbons and three cis double bonds. ALA is present in either cis ('Z') or trans ('E') conformation in the plants. Intake of ALA decrease the risk of cardiovascular diseases by 1) prevent recurrent ventricular arrhythmias that can lead to sudden cardiac death, 2) decrease risk of thrombosis (blood clot formation) that can lead to heart attack or stroke, 3) decrease serum triglyceride levels, 4) slow growth of atherosclerotic plaque, 5) improve vascular endothelial function, 6) lower blood pressure and 7) decrease inflammation^{27,28}. ALA deficiency may lead to visual impairment and sensory neuropathy, scaly and hemorrhagic skin or scalp inflammations.²⁷ Therefore PDO3FA has to be complemented through food or supplements to maintain the balance between omega-3 and omega-6. Clinical studies have shown that PDO3FA has a preventive and therapeutic effect for multiple sclerosis, anxiety, depression, dyslipidemia, coronary heart disease, metabolic syndrome, diabetes and cancer related complications.^{23,28}

Moringa oleifera is a traditional medicinal plant used in treating myriads of ailments and diseases including body pain, weakness, fever, asthma, cough, blood pressure, arthritis, diabetes, epilepsy, wound, and skin infection. Recently, its phytocompounds have been used to treat diseases like HIV/AIDs, chronic anemia, cancer, malaria and hemorrhage. Of its several species, *M. oleifera* is widely cultivated species due to its multifarious uses in the management of health and disease²⁹. *M. oleifera* is native to India, however, cultivated all over the world. The plant is a deciduous tree with brittle stem, whitish-gray corky bark with branches; leaves pale green, bipinnate/ tri-pinnate with opposite, ovate leaflets³⁰⁻³³. All parts of the plant including leaves, roots, pods, seeds, and flowers have been explored for their nutraceutical and pharmaceutical properties. Pharmacological studies indicate that extracts obtained from the plant have significant medicinal properties³⁴⁻⁵¹. Aim of this study is to bioprospect ALA from the leaves of MO for its molecular and biological properties. There is a growing interest in using ALA for a number of purposes related to health and disease, but there isn't enough reliable information to whether it might be practically helpful. This study provides the baseline ADMETox information to develop PDO3FA - ALA as a novel lead in drug discovery.

MATERIALS AND METHODS

In silico Drug-Likeliness and Bioactivity Prediction

The drug likeliness and bioactivity of selected molecule was analyzed using the Molinspiration server (<http://www.molinspiration.com>). Molinspiration tool is cheminformatics software that provides molecular properties as well as bioactivity prediction of compounds. In Molinspiration-based drug-likeness analysis, there are two important factors, including the lipophilicity level (log P) and polar surface area (PSA) directly associated with the pharmacokinetic properties (PK) of the compounds.⁵² In Molinspiration-based bioactivity analysis, the calculation of the bioactivity score of compounds toward GPCR ligands, ion channel modulators, kinase inhibitors, nuclear receptor ligands, protease inhibitors, and other enzyme targets were analyzed by Bayesian statistics.⁵³ This was carried out for G protein-coupled receptors (GPCR), ion channels, kinases, nuclear hormone receptors, proteases, and other enzymes (RdRp), are the major drug targets of most of the drugs.⁵⁴

In silico ADMET Analysis

SwissADME: is a Web tool that gives free access to a pool of fast yet robust predictive models for physicochemical properties, pharmacokinetics, druglikeness and medicinal chemistry friendliness, among which in-house proficient methods such as iLOGP (a physics-based model for lipophilicity) or the BOILED-Egg. It is the first online tool that enables ADME-related calculation for multiple molecules, allowing chemical library analysis and efficient lead optimization.⁵⁵ PK properties, such as Absorption, Distribution, Metabolism, Excretion, and Toxicity (ADMET), of fatty acids were predicted using admerSAR v2.0 server (<http://lmmecust.edu.cn/admetsar2/>) and admerSAR server is an open-source computational tool for prediction of ADMET properties of compounds, which makes it a practical platform for drug discovery and other pharmacological research. In ADMET analysis, absorption (A) of good drugs depends on factors such as membrane permeability [designated by colon cancer cell line (Caco-2)]⁵⁶, human intestinal absorption (HIA)⁵⁷, and status of either P-glycoprotein substrate or inhibitor⁵⁸. The distribution (D) of drugs mainly depends on the ability to cross blood-brain barrier (BBB)⁵⁹. The metabolism (M) of drugs is calculated by the CYP, MATE1, and OATP1B1-OATP1B3 models⁶⁰. Excretion (E) of drugs is estimated based on the renal OCT substrate. Toxicity (T) of drugs is predicted on Human Ether-A-Go-Go related gene inhibition, carcinogenic status, mutagenic status, and acute oral toxicity^{61,62}.

vNN model building and analysis

vNN method was used to calculate the similarity distance between molecules in terms of their structure, and uses a distance threshold to define a domain of applicability to ensure that the predictions generated are reliable. vNN models can be built keeping quantitative structure-activity relationship (QSAR) models up-to-date to maintain their performance levels. Performance characteristics of the models are comparable, and often superior to those of other more elaborate model.⁶³ One of the most widely used measures of similarity distance between two small molecules is Tanimoto distance, d, which is defined as:

$$d = 1 - \frac{n(P \cap Q)}{n(P) + n(Q) - (P \cap Q)}$$

where $n(P \cap Q)$ is number of features common to molecules p and q, and $n(P)$ and $n(Q)$ are the total numbers of features for molecules p and q, respectively. The predicted biological

activity y is given by a weighted across structurally similar neighbours:

$$y = \frac{\sum_{i=1}^v y_{ie} - (di/h)^2}{\sum_{i=1}^v - (di/h)^2} \quad di \leq d_0$$

where d_i denotes Tanimoto distance between a query molecule for which a prediction is made and a molecule i of the training set; d_0 is a Tanimoto-distance threshold, beyond which two molecules are no longer considered to be sufficiently similar to be included in the average; y_i is the experimentally measured activity of molecule i ; v denotes the total number of molecules in the training set that satisfies the condition $d_i \leq d_0$; and h is a smoothing factor, which dampens the distance penalty. Values of h and d_0 are determined from cross-validation studies. To identify structurally similar compounds, Accelrys extended-connectivity fingerprints with a diameter of four chemical bonds (ECFP4) was used which have previously been reported to show good overall performance.^{64,65}

Model Validation

A 10-fold cross-validation (CV) procedure was used to validate new models and to determine the values of smoothing factor h and Tanimoto distance d_0 . In this procedure, data was randomly divided into 10 sets, and used 9 to develop the model and 10th to validate it, this process was repeated 10 times, leaving each set of molecules out once.

Performance Measures

Following metrics were used to assess model performance. (1) sensitivity measures a model's ability to correctly detect true positives, (2) specificity measures a model's ability to detect true negatives, (3) accuracy measures a model's ability to make correct predictions and (4) kappa compares the probability of correct predictions to the probability of correct predictions by chance (its value ranges from +1 (perfect agreement between model prediction and experiment) to -1 (complete disagreement), with 0 indicating no agreement beyond that expected by chance).

$$\text{sensitivity} = \frac{\text{TP}}{\text{TP} + \text{FN}}$$

$$\text{specificity} = \frac{\text{TN}}{\text{FP} + \text{TN}}$$

$$\text{accuracy} = \frac{\text{TP} + \text{TN}}{\text{TP} + \text{TN} + \text{FP} + \text{FN}}$$

$$\text{kappa} = \frac{\text{accuracy} - \text{Pr}(e)}{1 - \text{Pr}(e)}$$

where TP, TN, FP, and FN denote the numbers of true positives, true negatives, false positives, and false negatives, respectively. Kappa is a metric for assessing the quality of binary classifiers. $\text{Pr}(e)$ is an estimate of the probability of a correct prediction by chance. It is calculated as:

$$\text{Pr}(e) = \frac{(\text{TP} + \text{FN})(\text{TP} + \text{FP}) + (\text{TP} + \text{FN})(\text{TP} + \text{FP})}{(\text{TP} + \text{FN} + \text{FP} + \text{TN})^2}$$

The coverage is the proportion of test molecules with at least one nearest neighbour that meets the similarity criterion. The coverage is a measure of how many test compounds are within the applicability domain of a prediction model.

RESULTS AND DISCUSSION

Chemical Kingdom	: Organic Compounds
Super Class	: Lipids and Lipid-like Molecules
Class	: Fatty Acyls
Subclass	: Lineolic acids and derivatives
IUPAC Name	: (9Z,12Z,15Z)-octadeca-9,12,15-trienoic acid
Common Name	: Linolenic Acid
Synonym	: (9,12,15)-linolenic acid
Compound CID	: 5280934
PubChem Identifier	: 5280934
ChEBI Identifier	: 25048
CAS Identifier	: 463-40-1
Molecular Formula	: C ₁₈ H ₃₀ O ₂
Molecular Weight	: 278.4g/mol
Canonical SMILES	: CC/C=C\C/C=C\C/C=C\CCCCC CC(=O)O
InChIKey	: DTOSIQBPPRVQHS- PDBXOOCHSA-N

3D structure, molecular and biological properties of PDO3FA-ALA in *M. oleifera*, its physicochemical properties, lipophilicity properties, water solubility properties, pharmacokinetic properties, druglikeness, medicinal chemistry properties⁶⁶, ADMET properties of ALA from *M. oleifera* is provided in Table 1-3 respectively. Performance measures of vNN models in 10-fold cross validation using a restricted/ unrestricted applicability domain for ALA from *M. oleifera* (Table 4).

ADMET Predictions

The implemented Absorption, Distribution, Metabolism, Excretion and Toxicity (ADMET) prediction models, including their performance measures, have been reported previously.^{62,63,67} The 15 models cover a diverse set of ADMET endpoints. Some of the models have already been published, including those for Maximum Recommended Therapeutic Dose (MRTD)⁶⁸, chemical mutagenicity⁶⁹, human liver microsomal (HLM)⁷⁰, Pgp inhibitor substrates⁷¹.

The implemented Absorption, Distribution, Metabolism, Excretion and Toxicity (ADMET) prediction models, including their performance measures, are available online. The 15 models cover a diverse set of ADMET endpoints. Models have included for Maximum Recommended Therapeutic Dose (MRTD), chemical mutagenicity, human liver microsomal (HLM), Pgp inhibitor substrates.

Query	Liver Toxicity		Metabolism						Membrane Transporters			Others			
			Cyp Inhibitors for						BBB	P-gp Inhibitor	P-gp Substrate	hERG Blocker	MMP	AMES	MRTD (mg/day)
	DILI	Cyto-toxicity	HLM	1A2	3A4	2D6	2C8	2C19							
	Yes	∅	∅	No	No	No	No	No	∅	No	No	Yes	No	No	20

Liver Toxicity - DILI: Drug-induced liver injury (DILI) has been one of the most commonly cited reasons for drug withdrawals from the market. This application predicts whether a compound could cause DILI. The dataset of 1,431 compounds was obtained from four sources. This dataset contains both pharmaceuticals and non-pharmaceuticals; a compound was classified as causing DILI if it was associated with a high risk of DILI and not if there was no such risk.

Cytotoxicity (HepG2): Cytotoxicity is the degree to which a chemical causes damage to cells. A cytotoxicity prediction model was developed using in vitro data on toxicity against HepG2 cells for 6,000 structurally diverse compounds, which was collected from ChEMBL. In developing the model, the compounds with an $IC_{50} \leq 10 \mu M$ were considered in the in vitro assay as cytotoxic.

Metabolism HLM: The human liver microsomal (HLM) stability assay is commonly used to identify and exclude compounds that are too rapidly metabolized. For a drug to achieve effective therapeutic concentrations in the body, it cannot be metabolized too rapidly by the liver. Compounds with a half-life of 30 min or longer in an HLM assay are considered as stable; otherwise they are considered unstable. HLM data was retrieved from the ChEMBL database, manually curated the data, and classified compounds as stable or unstable based on the reported half-life ($T_{1/2} > 30$ min was considered stable, and $T_{1/2} < 30$ min unstable). Final dataset contained 3,654 compounds. Of these, as much as 2,313 were classified as stable; 1,341 as unstable.

Cytochrome P450 enzyme (CYP) inhibition: CYPs constitute a superfamily of proteins that play an important role in the metabolism and detoxification of xenobiotics. In vitro data derived from five main drug-metabolizing CYPs - 1A2, 3A4, 2D6, 2C9, and 2C19 was used to develop CYP inhibition models. CYP inhibitors were retrieved from PubChem and classified a compound with an $IC_{50} \leq 10 \mu M$ for an enzyme as an inhibitor of the enzyme. Predictions for the following enzymes: CYP1A2, CYP3A4, CYP2D6, CYP2C9, and CYP2C19 has been provided.

Membrane Transporters - BBB: The blood-brain barrier (BBB) is a highly selective barrier that separates the circulating blood from the central nervous system. VNN-based BBB model has been developed, using 352 compounds whose BBB permeability values (log-BB) were obtained from the literature respectively^{72,73}. Compounds with logBB values of less than -0.3 and greater than +0.3 were classified as BBB non-permeable and permeable.

Pgp Substrates and Inhibitors: P-glycoprotein (Pgp) is an essential cell membrane protein that extracts many foreign substances from the cell. Cancer cells often overexpress Pgp, which increases the efflux of chemotherapeutic agents from the cell and prevents treatment by reducing the effective intracellular concentrations of such agents—a phenomenon known as multidrug resistance. For this reason, identifying compounds that can either be transported out of the cell by Pgp (substrates) or impair Pgp function (inhibitors) is of great interest. Models to predict both Pgp substrates and Pgp inhibitors were developed as mentioned by Xu et al.⁷⁴, and Schyman et al⁷⁵⁻⁷⁷. This dataset consists of measurements of 422 substrates and 400 non-substrates. To generate a large Pgp inhibitor dataset and both the datasets were combined⁷⁸ and removed duplicates to form a combined dataset consisting of 1,319 inhibitors/ 937 non-inhibitors⁷⁹.

hERG (Cardiotoxicity): The human ether-à-go-go-related gene (hERG) codes for a potassium ion channel involved in the normal cardiac repolarization activity of the heart. Drug-induced blockade of hERG function can cause long QT syndrome, which may result in arrhythmia and death. As much as 282 known hERG blockers from the literature were retrieved known hERG blockers from the literature and classified compounds

with an IC_{50} cut-off value of 10 μM or less as blockers. A set of 404 compounds with IC_{50} values greater than 10 μM were collected from ChEMBL and classified them as non-blockers⁷⁶.

MMP (Mitochondrial Toxicity): Given the fundamental role of mitochondria in cellular energetics and oxidative stress, mitochondrial dysfunction has been implicated in cancer, diabetes, neurodegenerative disorders, and cardiovascular diseases. A largest dataset of chemical-induced changes in mitochondrial membrane potential (MMP), was used based on the assumption that a compound that causes mitochondrial dysfunction is also likely to reduce the MMP. A vNN- model was developed based MMP prediction model, using 6,261 compounds collected from a previous study that screened a library of 10,000 compounds (~8,300 unique chemicals) at 15 concentrations, each in triplicate, to measure changes in the MMP in HepG2 cells. The study found that 913 compounds decreased the MMP, whereas 5,395 compounds had no effect as pointed out by Li et al.⁷⁷.

Mutagenicity (Ames test): Mutagens are chemicals that cause abnormal genetic mutations leading to cancer. A common way to assess a chemical's mutagenicity is the Ames test. A prediction model was developed using a literature dataset of 6,512 compounds, of which 3,503 were Ames-positive as indicated in previous study.³¹

MRTD: Maximum Recommended Therapeutic Dose (MRTD) is an estimated upper daily dose that is safe. A prediction model was developed based on a dataset of MRTD values publicly disclosed by the FDA, mostly of single-day oral doses for an average adult with a body weight of 60 kg, for 1,220 compounds (most of which are small organic drugs). Organometallics, high-molecular weight polymers were excluded (>5,000 Da), nonorganic chemicals, mixtures of chemicals, and very small molecules (<100 Da). An external test set of 160 compounds collected by the FDA was used for validation. The total dataset for the model contained 1,185 compounds⁶⁸. The predicted MRTD value for O3FA (mg/day unit) was calculated based upon an average adult weighing 60 kg.

Target - Probability Prediction: Cyclooxygenase-1 (PTGS1) - 0.859; Peroxisome proliferator-activated receptor gamma (PPARG) - 0.555; Peroxisome proliferator-activated receptor alpha (PPARA) - 0.555; Fatty acid binding protein muscle (FABP3) - 0.538; Free fatty acid receptor 1 (FFAR1) - 0.520; Fatty acid binding protein adipocyte (FABP4) - 0.520; Peroxisome proliferator-activated receptor delta (PPARD) - 0.520; Fatty acid binding protein epidermal (FABP5) - 0.182; Anandamide amidohydrolase (FAAH) - 0.164; Telomerase reverse transcriptase (TERT) - 0.147; Fatty acid-binding protein, liver (FABP1) - 0.112; Cannabinoid receptor 1 (CNR1) - 0.104; Acyl-CoA desaturase (SCD) - 0.095; Protein-tyrosine phosphatase 1B (PTPN1) - 0.095; DNA polymerase beta (POLB) - 0.095; Arachidonate 5-lipoxygenase (ALOX5) - 0.095; T-cell protein-tyrosine phosphatase (PTPN2) - 0.095; Prostaglandin E synthase (PTGES) - 0.095; Leukotriene B4 receptor 1 (LTB4R) - 0.095; Carboxylesterase 2 (CES2) - 0.095; Estrogen receptor beta (ESR2) - 0.086; Protein-tyrosine phosphatase 1C (PTPN6) - 0.086; Protein farnesyltransferase (FNTA FNTB) - 0.086; Nuclear receptor ROR-gamma (RORC) - 0.078; Arachidonate 12-lipoxygenase (ALOX12) - 0.078; 11-beta-hydroxysteroid dehydrogenase 1 (HSD11B1) - 0.078; DNA topoisomerase I (TOP1) - 0.078; Prostanoid IP receptor (PTGIR) - 0.078; Phosphodiesterase 4D (PDE4D) - 0.069; Nitric oxide synthase, inducible (NOS2) - 0.069; Prostanoid EP2 receptor (by homology) (PTGER2) - 0.069; Dual specificity phosphatase Cdc25A (CDC25A) - 0.069; Cytochrome P450 19A1 (CYP19A1) - 0.060; Glucocorticoid receptor (NR3C1) - 0.060; Vanilloid receptor (TRPV1) - 0.060; CD81 antigen (CD81) - 0.060; Protein kinase C eta (PRKCH) - 0.060; Receptor-type tyrosine-protein phosphatase F (LAR) (PTPRF) - 0.060; LXR-alpha (NR1H3) -

0.060; Corticosteroid binding globulin (SERPINA6) - 0.060; Testis-specific androgen-binding protein (SHBG) - 0.060; Glucose-6-phosphate 1-dehydrogenase (G6PD) - 0.060; Cytochrome P450 51 (by homology) (CYP51A1) - 0.060. G protein-coupled receptor 44 (PTGDR2) - 0.060; Protein-tyrosine phosphatase 2C (PTPN11) - 0.060; Low molecular weight phosphotyrosine protein (ACP1) - 0.060; Phospholipase A2 group 1B (PLA2G1B) - 0.060; Steroid 5-alpha-reductase 2 (SRD5A2) - 0.060; Prostanoid EP1 receptor (PTGER1) - 0.060; Estrogen receptor alpha (ESR1) - 0.060; G-protein coupled receptor 120 (FFAR4) - 0.060; HMG-CoA reductase (HMGCR) - 0.060; Niemann-Pick C1-like protein 1 (NPC1L1) - 0.060; Sigma opioid receptor (SIGMAR1) - 0.060; Cytochrome P450 17A1 (CYP17A1) - 0.060; Prostanoid EP4 receptor (PTGER4) - 0.060; Dual specificity phosphatase Cdc25B (CDC25B) - 0.060; Monocarboxylate transporter 1 (by homology) (SLC16A1) - 0.060; Interleukin-6 (IL6) - 0.060; Glutamine synthetase (GLUL) - 0.060; 11-beta-hydroxysteroid dehydrogenase 2 (HSD11B2) - 0.060; Mineralocorticoid receptor (NR3C2) - 0.060; Adenosine A3 receptor (ADORA3) - 0.060; Cyclooxygenase-2 (PTGS2) - 0.060; G-protein coupled bile acid receptor 1 (GPBAR1) - 0.060; Androgen Receptor (AR) - 0.060; MAP kinase ERK1 (MAPK3) - 0.060; Progesterone receptor (PGR) - 0.060; Prolyl endopeptidase (PREP) - 0.060; Autotaxin (ENPP2) - 0.060; Endothelin receptor ET-A (by homology) (EDNRA) - 0.060; Matrix metalloproteinase 13 (MMP13) - 0.060; Matrix metalloproteinase 3 (MMP3) - 0.060; Matrix metalloproteinase 8 (MMP8) - 0.060; Butyrylcholinesterase (BCHE) - 0.060; Cytosolic phospholipase A2 (PLA2G4A) - 0.060; Cytochrome P450 26B1 (CYP26B1) - 0.060; Cytochrome P450 26A1 (CYP26A1) - 0.060 respectively (Table 5; Figure 1).

CONCLUSION

In the present study ALA from *M. oleifera* was ADMET predicted for functional target oriented properties. It has been well established that in the human system, ALA is converted to EPA/DHA. EPA/ DHA endowed with cardioprotective potentials lowers blood cholesterol level and reduces the risk of heart disease. With limited data, it is not obvious to conclude that ALA of MO is safe as a dietary ingredient as evidence on risks associated with ALA remains inadequate as of now. *In-silico* ADMET prediction data presented in the paper is hopefully expected to assist the process of drug discovery by rapid design, evaluation, and prioritization of ALA owing to its remarkable biomedical applications.

REFERENCES

- Ponnampalam EN, Sinclair AJ, Holman BW. The sources, synthesis and biological actions of omega-3 and omega-6 fatty acids in red meat: An overview. *Foods*. 2021; 10(6):1358. <https://doi.org/10.3390/foods10061358>
- Saini RK, Keum YS. Omega-3 and omega-6 polyunsaturated fatty acids: Dietary sources, metabolism, and significance-A review. *Life sciences*. 2018; 203:255-67. <https://doi.org/10.1016/j.lfs.2018.04.049>
- Prasad P, Anjali P, Sreedhar RV. Plant-based stearidonic acid as sustainable source of omega-3 fatty acid with functional outcomes on human health. *Critical Reviews in Food Science and Nutrition*. 2021; 61(10):1725-37. <https://doi.org/10.1080/10408398.2020.1765137>
- Ringseis R, Müller A, Herter C, Gahler S, Steinhart H, Eder K. CLA isomers inhibit TNF α -induced eicosanoid release from human vascular smooth muscle cells via a PPAR γ ligand-like action. *Biochimica et Biophysica Acta (BBA)-General Subjects*. 2006; 1760(2):290-300. <https://doi.org/10.1016/j.bbagen.2005.12.002>
- Prasad P, Anjali P, Sreedhar RV. Plant-based stearidonic acid as sustainable source of omega-3 fatty acid with functional outcomes on human health. *Critical Reviews in Food Science and Nutrition*. 2021; 61(10):1725-37. <https://doi.org/10.1080/10408398.2020.1765137>
- Baker EJ, Valenzuela CA, De Souza CO, Yaqoob P, Miles EA, Calder PC. Comparative anti-inflammatory effects of plant-and marine-derived omega-3 fatty acids explored in an endothelial cell line. *Biochimica et Biophysica Acta (BBA)-Molecular and Cell Biology of Lipids*. 2020; 1865(6):158662. <https://doi.org/10.1016/j.bbaply.2020.158662>
- Whelan J. Dietary stearidonic acid is a long chain (n-3) polyunsaturated fatty acid with potential health benefits. *Journal of Nutrition*. 2009; 139(1):5-10. <https://doi.org/10.3945/jn.108.094268>
- Dyall SC. Long-chain omega-3 fatty acids and the brain: a review of the independent and shared effects of EPA, DPA and DHA. *Frontiers in aging neuroscience*. 2015; 7:52. <https://doi.org/10.3389/fnagi.2015.00052>
- Rainsford KD, Ying C, Smith FC. Effects of meloxicam, compared with other NSAIDs, on cartilage proteoglycan metabolism, synovial prostaglandin E2, and production of interleukins 1, 6 and 8, in human and porcine explants in organ culture. *Journal of Pharmacy and Pharmacology*. 1997 Oct; 49(10):991-8. <https://doi.org/10.1111/j.2042-7158.1997.tb06030.x>
- Michaelsen N, Sadybekov A, Besserer-Offroy É, Han GW, Krishnamurthy H, Zamlynny BA, Fradera X, Siliphaitvanh P, Presland J, Spencer KB, Soisson SM. Structural insights on ligand recognition at the human leukotriene B4 receptor 1. *Nature communications*. 2021; 12(1):1-2. <https://doi.org/10.1038/s41467-021-23149-1>
- Ferraz CR, Manchope MF, Andrade KC, Saraiva-Santos T, Franciosi A, Zaninelli TH, Bagatim-Souza J, Borghi SM, Cândido DM, Knysak I, Casagrande R. Peripheral mechanisms involved in *Tityus bahiensis* venom-induced pain. *Toxicon*. 2021; 200:3-12. <https://doi.org/10.1016/j.toxicon.2021.06.013>
- Patel A, Karageorgou D, Katapodis P, Sharma A, Rova U, Christakopoulos P, Matsakas L. Bioprospecting of thraustochytrids for omega-3 fatty acids: A sustainable approach to reduce dependency on animal sources. *Trends in Food Science & Technology*. 2021; 115:433-44. <https://doi.org/10.1016/j.tifs.2021.06.044>
- Fisk HL, Childs CE, Miles EA, Ayres R, Noakes PS, Paras-Chavez C, Kuda O, Kopecký J, Antoun E, Lillycrop KA, Calder PC. Modification of subcutaneous white adipose tissue inflammation by omega-3 fatty acids is limited in human obesity-a double blind, randomised clinical trial. *EBioMedicine*. 2022; 77:103909. <https://doi.org/10.1016/j.ebiom.2022.103909>
- Albracht-Schulte K, Kalupahana NS, Ramalingam L, Wang S, Rahman SM, Robert-McComb J, Moustaid-Moussa N. Omega-3 fatty acids in obesity and metabolic syndrome: a mechanistic update. *The Journal of nutritional biochemistry*. 2018; 58:1-6. <https://doi.org/10.1016/j.jnutbio.2018.02.012>
- Nguyen QV, Malau-Aduli BS, Cavalieri J, Nichols PD, Malau-Aduli AE. Enhancing omega-3 long-chain polyunsaturated fatty acid content of dairy-derived foods for human consumption. *Nutrients*. 2019 Apr; 11(4):743. <https://doi.org/10.3390/nu11040743>
- Gutiérrez S, Svahn SL, Johansson ME. Effects of omega-3 fatty acids on immune cells. *International journal of molecular sciences*. 2019 Jan; 20(20):5028. <https://doi.org/10.3390/ijms20205028>
- Yan, Y.; Jiang, W.; Spinetti, T.; Tardivel, A.; Castillo, R.; Bourquin, C.; Guarda, G.; Tian, Z.; Tschopp, J.; Zhou, R. Omega-3 fatty acids prevent inflammation and metabolic disorder through inhibition of NLRP3 inflammasome activation. *Immunity* 2013, 38, 1154-1163. <https://doi.org/10.1016/j.immuni.2013.05.015>
- Das UN. Biological significance of essential fatty acids. *Journal- Association Of Physicians of India*. 2006 Apr 1; 54(R):309.
- Zhu X, Wang B, Zhang X, Chen X, Zhu J, Zou Y, Li J. Alpha-linolenic acid protects against lipopolysaccharide-induced acute lung injury through anti-inflammatory and anti-oxidative pathways. *Microbial Pathogenesis*. 2020 May 1; 142:104077. <https://doi.org/10.1016/j.micpath.2020.104077>
- Czumaj A, Śledziński T. Biological role of unsaturated fatty acid desaturases in health and disease. *Nutrients*. 2020 Feb; 12(2):356. <https://doi.org/10.3390/nu12020356>
- Monroig Ó, Shu-Chien AC, Kabeya N, Tocher DR, Castro LF. Desaturases and elongases involved in long-chain polyunsaturated

fatty acid biosynthesis in aquatic animals: From genes to functions. *Progress in Lipid Research*. 2022 Jan 31:101157. <https://doi.org/10.1016/j.plipres.2022.101157>

22. Gocen T, Bayarlı SH, Guven MH. Effects of chemical structures of omega-6 fatty acids on the molecular parameters and quantum chemical descriptors. *Journal of Molecular Structure*. 2018 Dec 15; 1174:142-50. <https://doi.org/10.1016/j.molstruc.2018.04.075>

23. Çetin Z, Saygili El, Benlier N, Ozkurn M, Sayin S. Omega-3 Polyunsaturated Fatty Acids and Cancer. In *Nutraceuticals and Cancer Signalling* (pp. 591-631). Springer, Cham. https://doi.org/10.1007/978-3-030-74035-1_22

24. Kaur KK, Allahbadia G, Singh M. Synthesis and functional significance of poly unsaturated fatty acids (PUFA's) in body. *Acta Scientific Nutritional Health*. 2018; 2(4):8.

25. Varela-López A, Vera-Ramírez L, Giampieri F, Navarro-Hortal MD, Forbes-Hernández TY, Battino M, Quiles JL. The central role of mitochondria in the relationship between dietary lipids and cancer progression. *InSeminars in Cancer Biology* 2021; 73:86-100. Academic Press. <https://doi.org/10.1016/j.semancer.2021.01.001>

26. Wiktorowska-Owczarek A, Berezinska M, Nowak JZ. PUFAs: structures, metabolism and functions. *Adv Clin Exp Med*. 2015 Nov 1; 24(6):931-41. <https://doi.org/10.17219/acem/31243>

27. Lau AT, Yu FY, Xu YM. Epigenetic effects of essential fatty acids. *Current Pharmacology Reports*. 2019 Feb; 5(1):68-78. <https://doi.org/10.1007/s40495-019-00166-9>

28. Mozaffarian D, Wu JH. Omega-3 fatty acids and cardiovascular disease: effects on risk factors, molecular pathways, and clinical events. *Journal of the American College of Cardiology*. 2011; 58(20):2047-67. <https://doi.org/10.1016/j.jacc.2011.06.063>

29. Sujatha BK, Patel P. Moringa Oleifera-Nature's Gold. *Imperial Journal of Interdisciplinary Research*. 2017; 3(5):1175-9.

30. Saini RK, Sivanesan I, Keum YS. Phytochemicals of Moringa oleifera: a review of their nutritional, therapeutic and industrial significance. *3 Biotech* 2016; 6(2):1-4. <https://doi.org/10.1007/s13205-016-0526-3>

31. Parvathi K, Kandeepan C, Sabitha M, Senthilkumar N, Ramya S, Boopathi NM, Ramanathan L, Jayakumararaj R, In-silico Absorption, Distribution, Metabolism, Elimination and Toxicity profile of 9,12,15-Octadecatrienoic acid (ODA) from Moringa oleifera, *Journal of Drug Delivery and Therapeutics*. 2022; 12(2-s):142-150 <https://doi.org/10.22270/jddt.v12i2-S.5289>

32. Kashyap P, Kumar S, Riar CS, Jindal N, Baniwal P, Guiné RP, Correia PM, Mehra R, Kumar H. Recent Advances in Drumstick (Moringa oleifera) Leaves Bioactive Compounds: Composition, Health Benefits, Bioaccessibility, and Dietary Applications. *Antioxidants*. 2022; 11(2):402. <https://doi.org/10.3390/antiox11020402>

33. Al-Ghanayem AA, Alhussaini MS, Asad M, Joseph B. Moringa oleifera Leaf Extract Promotes Healing of Infected Wounds in Diabetic Rats: Evidence of Antimicrobial, Antioxidant and Proliferative Properties. *Pharmaceuticals*. 2022; 15(5):528. <https://doi.org/10.3390/ph15050528>

34. Ramya S, Neethirajan K, Jayakumararaj R. Profile of bioactive compounds in *Syzygium cumini*-a review. *Journal of Pharmacy research*. 2012; 5(8):4548-53.

35. Sundari A, Jayakumararaj R. Herbal remedies used to treat skin disorders in Arasankulam region of Thoothukudi District in Tamil Nadu, India. *Journal of Drug Delivery and Therapeutics*. 2020; 10(5):33-8. <https://doi.org/10.22270/jddt.v10i5.4277>

36. Sundari A, Jayakumararaj R. Medicinal plants used to cure cuts and wounds in Athur region of Thoothukudi district in Tamil Nadu, India. *Journal of Drug Delivery and Therapeutics*. 2020; 10(6-s):26-30. <https://doi.org/10.22270/jddt.v10i6-s.4429>

37. Kandeepan C, Kalaimathi RV, Jeevalatha A, Basha AN, Ramya S, Jayakumararaj R, In-silico ADMET Pharmacoinformatics of Geraniol (3,7-dimethyl octa-trans-2,6-dien-1-ol) - acyclic monoterpene alcohol drug from Leaf Essential Oil of *Cymbopogon martinii* from Sirumalai Hills (Eastern Ghats), INDIA, *Journal of Drug Delivery and Therapeutics*. 2021; 11(4-S):109-118 <https://doi.org/10.22270/jddt.v11i4-S.4965>

38. Loganathan T, Barathinivas A, Soorya C, Balamurugan S, Nagajothi TG, Ramya S, Jayakumararaj R, Physicochemical, Druggable, ADMET Pharmacoinformatics and Therapeutic Potentials of Azadirachta indica A. Juss., *Journal of Drug Delivery and Therapeutics*. 2021; 11(5):33-46 <https://doi.org/10.22270/jddt.v11i5.4981>

39. Loganathan T, Barathinivas A, Soorya C, Balamurugan S, Nagajothi TG, Ramya S, Jayakumararaj R, GCMS Profile of Bioactive Secondary Metabolites with Therapeutic Potential in the Ethanolic Leaf Extracts of Azadirachta indica: A Sacred Traditional Medicinal Plant of INDIA *Journal of Drug Delivery and Therapeutics*. 2021; 11(4-S):119-126 <https://doi.org/10.22270/jddt.v11i4-S.4967>

40. Sabitha M, Krishnaveni K, Murugan M, Basha AN, Pallan GA, Kandeepan C, Ramya S, Jayakumararaj R, In-silico ADMET predicated Pharmacoinformatics of Quercetin-3-Galactoside, polyphenolic compound from Azadirachta indica, a sacred tree from Hill Temple in Alagarkovil Reserve Forest, Eastern Ghats, INDIA, *Journal of Drug Delivery and Therapeutics*. 2021; 11(5-S):77-84 <https://doi.org/10.22270/jddt.v11i5-S.5026>

41. Soorya C, Balamurugan S, Basha AN, Kandeepan C, Ramya S, Jayakumararaj R, Profile of Bioactive Phytocompounds in Essential Oil of *Cymbopogon martinii* from Palani Hills, Western Ghats, INDIA, *Journal of Drug Delivery and Therapeutics*. 2021; 11(4):60-65 <https://doi.org/10.22270/jddt.v11i4.4887>

42. Soorya C, Balamurugan S, Ramya S, Neethirajan K, Kandeepan S, Jayakumararaj R, Physicochemical, ADMET and Druggable properties of Myricetin: A Key Flavonoid in *Syzygium cumini* that regulates metabolic inflammations, *Journal of Drug Delivery and Therapeutics*. 2021; 11(4):66-73 <https://doi.org/10.22270/jddt.v11i4.4890>

43. Jeevalatha A, Kalaimathi RV, Basha AN, Kandeepan C, Ramya S, Loganathan T, Jayakumararaj R, Profile of bioactive compounds in *Rosmarinus officinalis*, *Journal of Drug Delivery and Therapeutics*. 2022; 12(1):114122 <https://doi.org/10.22270/jddt.v12i1.5189>

44. Kalaimathi RV, Jeevalatha A, Basha AN, Kandeepan C, Ramya S, Loganathan T, Jayakumararaj R, In-silico Absorption, Distribution, Metabolism, Elimination and Toxicity profile of Isopulegol from *Rosmarinus officinalis*, *Journal of Drug Delivery and Therapeutics*. 2022; 12(1):102-108 <https://doi.org/10.22270/jddt.v12i1.5188>

45. Kandeepan C, Sabitha M, Parvathi K, Senthilkumar N, Ramya S, Boopathi NM, Jayakumararaj R, Phytochemical Screening, GCMS Profile, and In-silico properties of Bioactive Compounds in Methanolic Leaf Extracts of Moringa oleifera, *Journal of Drug Delivery and Therapeutics*. 2022; 12(2):87-99 <https://doi.org/10.22270/jddt.v12i2.5250>

46. Krishnaveni K, Sabitha M, Murugan M, Kandeepan C, Ramya S, Loganathan T, Jayakumararaj R, vNN model cross validation towards Accuracy, Sensitivity, Specificity and kappa performance measures of β -caryophyllene using a restricted unrestricted applicability domain on Artificial Intelligence & Machine Learning approach based in-silico prediction of ADMET properties, *Journal of Drug Delivery and Therapeutics*. 2022; 12(1s):123-131 <https://doi.org/10.22270/jddt.v12i1-S.5222>

47. Parvathi K, Kandeepan C, Sabitha M, Senthilkumar N, Ramya S, Boopathi NM, Ramanathan L, Jayakumararaj R, In-silico Absorption, Distribution, Metabolism, Elimination and Toxicity profile of 9,12,15-Octadecatrienoic acid (ODA) from Moringa oleifera, *Journal of Drug Delivery and Therapeutics*. 2022; 12(2-s):142-150 <https://doi.org/10.22270/jddt.v12i2-S.5289>

48. Ramya S, Loganathan T, Chandran M, Priyanka R, Kavipriya K, Grace Lydial Pushpalatha G, Aruna D, Abraham GC, Jayakumararaj R, ADME-Tox profile of Cuminaldehyde (4-Isopropylbenzaldehyde) from *Cuminum cyminum* seeds for potential biomedical applications, *Journal of Drug Delivery and Therapeutics*. 2022; 12(2-s):127-141 <https://doi.org/10.22270/jddt.v12i2-S.5286>

49. Ramya S, Loganathan T, Chandran M, Priyanka R, Kavipriya K, Grace Lydial Pushpalatha G, Aruna D, Ramanathan L, Jayakumararaj R, Phytochemical Screening, GCMS, FTIR profile of Bioactive Natural Products in the methanolic extracts of *Cuminum cyminum* seeds and oil, *Journal of Drug Delivery and Therapeutics*. 2022; 12(2-s):110-118 <https://doi.org/10.22270/jddt.v12i2-S.5280>

50. Ramya S, Murugan M, Krishnaveni K, Sabitha M, Kandeepan C, Jayakumararaj R, In-silico ADMET profile of Ellagic Acid from *Syzygium cumini*: A Natural Biaryl Polyphenol with Therapeutic Potential to Overcome Diabetic Associated Vascular Complications. *Journal of Drug Delivery and Therapeutics*. 2022; 12(1):91-101 <https://doi.org/10.22270/jddt.v12i1.5179>

51. Ramya S, Soorya C, Sundari A, Grace Lydial Pushpalatha G, Aruna D, Loganathan T, Balamurugan S, Abraham GC, Ponrathy T, Kandeepan C, Jayakumararaj R, Artificial Intelligence and Machine Learning approach based in-silico ADME-Tox and Pharmacokinetic Profile of α -Linolenic acid from *Catharanthus roseus* (L.) G. Don., *Journal of Drug Delivery and Therapeutics*. 2022; 12(2-s):96-109 <https://doi.org/10.22270/jddt.v12i2-S.5274>

52. Beetge E, du Plessis J, Müller DG, Goosen C, van Rensburg FJ. The influence of the physicochemical characteristics and pharmacokinetic properties of selected NSAID's on their transdermal absorption. *International journal of Pharmaceutics*. 2000; 193(2):261-4. [https://doi.org/10.1016/S0378-5173\(99\)00340-3](https://doi.org/10.1016/S0378-5173(99)00340-3)

53. Mabkhot YN, Alatibi F, El-Sayed NN, Al-Showiman S, Kheder NA, Wadood A, Rauf A, Bawazeer S, Hadda TB. Antimicrobial activity of some novel armed thiophene derivatives and petra/osiris/molinspiration (POM) analyses. *Molecules*. 2016; 21(2):222. <https://doi.org/10.3390/molecules21020222>

54. Hauser AS, Attwood MM, Rask-Andersen M, Schiöth HB, Gloriam DE. Trends in GPCR drug discovery: new agents, targets and indications. *Nature reviews Drug discovery*. 2017 Dec; 16(12):829-42. <https://doi.org/10.1038/nrd.2017.178>

55. Daina A, Michielin O, Zoete V. SwissADME: a free web tool to evaluate pharmacokinetics, drug-likeness and medicinal chemistry friendliness of small molecules. *Scientific reports*. 2017; 7(1):1-3 <https://doi.org/10.1038/srep42717>

56. Hubatsch I, Ragnarsson EG, Artursson P. Determination of drug permeability and prediction of drug absorption in Caco-2 monolayers. *Nature protocols*. 2007; 2(9):2111-9. <https://doi.org/10.1038/nprot.2007.303>

57. Radchenko EV, Dyabina AS, Palyulin VA, Zefirov NS. Prediction of human intestinal absorption of drug compounds. *Russian Chemical Bulletin*. 2016; 65(2):576-80. <https://doi.org/10.1007/s11172-016-1340-0>

58. Alam A, Kowal J, Broude E, Roninson I, Locher KP. Structural insight into substrate and inhibitor discrimination by human P-glycoprotein. *Science*. 2019; 363(6428):753-6. <https://doi.org/10.1126/science.aav7102>

59. Daina A, Zoete V. A boiled-egg to predict gastrointestinal absorption and brain penetration of small molecules. *ChemMedChem*. 2016; 11(11):1117-21. <https://doi.org/10.1002/cmdc.201600182>

60. Liao M, Jaw-Tsai S, Beltman J, Simmons AD, Harding TC, Xiao JJ. Evaluation of in vitro absorption, distribution, metabolism, and excretion and assessment of drug-drug interaction of rucaparib, an orally potent poly (ADP-ribose) polymerase inhibitor. *Xenobiotica*. 2020; 50(9):1032-42. <https://doi.org/10.1080/00498254.2020.1737759>

61. Jia CY, Li JY, Hao GF, Yang GF. A drug-likeness toolbox facilitates ADMET study in drug discovery. *Drug Discovery Today*. 2020; 25(1):248-58. <https://doi.org/10.1016/j.drudis.2019.10.014>

62. Cheng F, Li W, Zhou Y, Shen J, Wu Z, Liu G, Lee PW, Tang Y. *admetSAR*: a comprehensive source and free tool for assessment of chemical ADMET properties.

63. Schyman, P., R. Liu, and A. Wallqvist. Using the variable-nearest neighbor method to identify P-glycoprotein substrates and inhibitors. *ACS Omega*. 2016; 1(5):923-929 <https://doi.org/10.1021/acsomega.6b00247>

64. Rogers, D., and M. Hahn. Extended-connectivity fingerprints. *Journal of Chemical Information and Modelling*. 2010; 50(5):742-754 <https://doi.org/10.1021/ci100050t>

65. Duan, J., S. Dixon, J. Lowrie, and W. Sherman. Analysis and comparison of 2D fingerprints: Insights into database screening performance using eight fingerprint methods. 2010; 29(2):157-170 <https://doi.org/10.1016/j.jmgm.2010.05.008>

66. Alnajjar R, Mohamed N, Kawafi N. Bicyclo Pentane as phenyl substituent in atorvastatin drug to improve physicochemical properties: drug-likeness, DFT, pharmacokinetics, docking, and molecular dynamic simulation. *Journal of Molecular Structure*. 2021; 1230:129628 <https://doi.org/10.1016/j.molstruc.2020.129628>

67. Schyman, P., R. Liu, V. Desai, and A. Wallqvist. vNN web server for ADMET predictions. *Frontiers in Pharmacology*. 2017 December 4; 8:889. <https://doi.org/10.3389/fphar.2017.00889>

68. Liu, R., G. Tawa, and A. Wallqvist. Locally weighted learning methods for predicting dose-dependent toxicity with application to the human maximum recommended daily dose. *Chemical Research in Toxicology*. 2012; 25(10):2216-2226. <https://doi.org/10.1021/tx300279f>

69. Liu, R., and A. Wallqvist. Merging applicability domains for in silico assessment of chemical mutagenicity. *Journal of Chemical Information and Modeling*. 2014; 54(3):793-800. <https://doi.org/10.1021/ci500016v>

70. Liu, R., P. Schyman, and A. Wallqvist. Critically assessing the predictive power of QSAR models for human liver microsomal stability. *Journal of Chemical Information and Modeling*. 2015; 55(8):1566-1575. <https://doi.org/10.1021/acs.jcim.5b00255>

71. Schyman, P., R. Liu, and A. Wallqvist. Using the variable-nearest neighbor method to identify P-glycoprotein substrates and inhibitors. *ACS Omega*. 2016; 1(5):923-929. <https://doi.org/10.1021/acsomega.6b00247>

72. Muehlbacher, M., G. Spitzer, K. Liedl, J. Kornhuber. Qualitative prediction of blood-brain barrier permeability on a large and refined dataset. *Journal of Computer-Aided Molecular Design*. 2011; 25:1095. <https://doi.org/10.1007/s10822-011-9478-1>

73. Naef R. A generally applicable computer algorithm based on the group additivity method for the calculation of seven molecular descriptors: heat of combustion, logPO/W, logS, refractivity, polarizability, toxicity and logBB of organic compounds; scope and limits of applicability. *Molecules*. 2015; 20(10):18279-18351 <https://doi.org/10.3390/molecules201018279>

74. Xu, Y., Z. Dai, F. Chen, S. Gao, J. Pei, and L. Lai. Deep learning for drug-induced liver injury. 2015, 55(10):2085-2093. <https://doi.org/10.1021/acs.jcim.5b00238>

75. Schyman, P., R. Liu, and A. Wallqvist. General purpose 2D and 3D similarity approach to identify hERG blockers. *Journal of Chemical Information and Modeling*. 2016; 56(1):213-222 <https://doi.org/10.1021/acs.jcim.5b00616>

76. Attene-Ramos, M., R. Huang, S. Michael, K. Witt, A. Richard, R. Tice, A. Simeonov, C. Austin, M. Xia. Profiling of the Tox21 chemical collection for mitochondrial function to identify compounds that acutely decrease mitochondrial membrane potential. 2015; 123(1):49 <https://doi.org/10.1289/ehp.1408642>

77. Li, D., L. Chen, Y. Li, S. Tian, H. Sun, and T. Hou. ADMET evaluation in drug discovery. Development of in Silico prediction models for P-Glycoprotein substrates. 2014; 11(3):716-726. <https://doi.org/10.1021/mp400450m>

78. Broccatelli, F., E. Carosati, A. Neri, M. Frosini, L. Goracci, T. Oprea, and G. Cruciani. A novel approach for predicting P-Glycoprotein (ABCB1) inhibition using molecular interaction fields. 2011; 54(6):1740-1751. <https://doi.org/10.1021/jm101421d>

79. Chen, L., Y. Li, Q. Zhao, H. Peng, and T. Hou. ADME evaluation in drug discovery. 10. Predictions of P-Glycoprotein inhibitors using recursive partitioning and naive bayesian classification techniques. 2011; 8(3):889-900. <https://doi.org/10.1021/mp100465q>

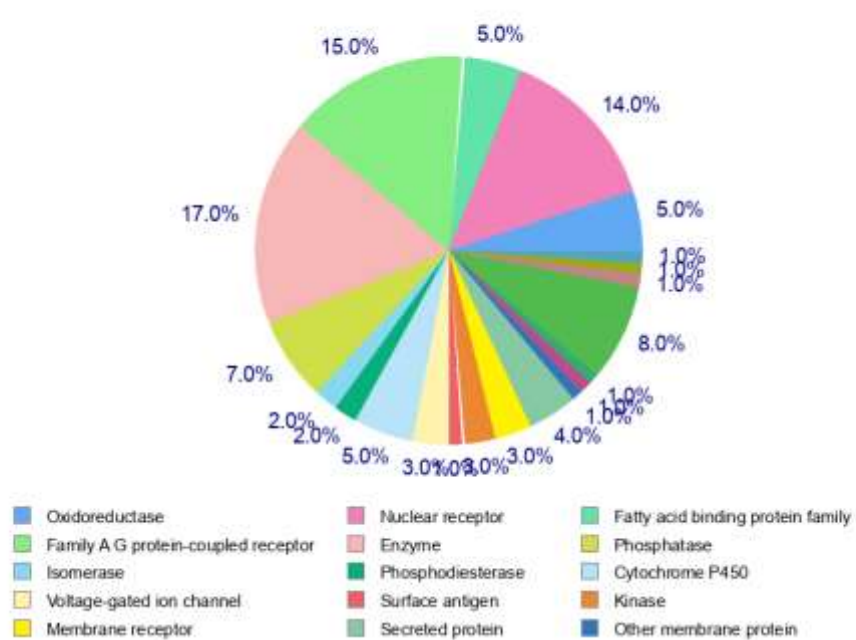


Figure 1: Percentage Target Probability of ALA from *Moringa oleifera*

Table 1 Physicochemical, Lipophilicity, Solubility, Pharmacokinetics and Drug likeness properties of LA

Physicochemical Properties	
Formula	C18H30O2
Molecular weight	278.43 g/mol
Num. heavy atoms	20
Num. arom. heavy atoms	0
Fraction Csp3	0.61
Num. rotatable bonds	13
Num. H-bond acceptors	2
Num. H-bond donors	1
Molar Refractivity	88.99
TPSA	37.30 Å ²
Lipophilicity	
Log Po/w (iLOGP)	4.30
Log Po/w (XLOGP3)	8.23
Log Po/w (WLOGP)	5.66
Log Po/w (MLOGP)	4.67
Log Po/w (SILICOS-IT)	6.13
Consensus Log Po/w	5.93
Water Solubility	
Log S (ESOL)	-5.73
Solubility	5.26e-04 mg/ml ; 1.85e-06 mol/l
Class	Moderately soluble
Log S (Ali)	-8.87
Solubility	3.80e-07 mg/ml ; 1.33e-09 mol/l
Class	Poorly soluble
Log S (SILICOS-IT)	-6.11
Solubility	2.19e-04 mg/ml ; 7.71e-07 mol/l
Class	Poorly soluble
Pharmacokinetics	
GI absorption	High
BBB permeant	No
P-gp substrate	No
CYP1A2 inhibitor	Yes
CYP2C19 inhibitor	No
CYP2C9 inhibitor	No
CYP2D6 inhibitor	No
CYP3A4 inhibitor	No
Log K _p (skin permeation)	-2.19 cm/s
Druglikeness	
Lipinski	Yes; 1 violation: MLOGP>4.15
Ghose	No; 1 violation: WLOGP>5.6
Veber	No; 1 violation: Rotors>10
Egan	No; 1 violation: WLOGP>5.88
Muegge	No; 2 violations: XLOGP3>5, Rotors>15
Bioavailability Score	0.85
Medicinal Chemistry	
PAINS	0 alert
Brenk	0 alert
Leadlikeness	No; 2 violations: Rotors>7, XLOGP3>3.5
Synthetic accessibility	2.54

Table 2: Summary of Physicochemical, Druggability & ADMET properties of LA

Physicochemical Properties Property	
Molecular weight	278.44 g/mol
LogP	5.66
LogD	3.68
LogSw	-4.78
Number of stereocenters	0
Stereochemical complexity	0.000
Fsp3	0.611
Topological polar surface area	37.30 Å ²
Number of hydrogen bond donors	1
Number of hydrogen bond acceptors	1
Number of smallest set of smallest rings (SSSR)	0
Size of the biggest system ring	0
Number of rotatable bonds	13
Number of rigid bonds	4
Number of charged groups	1
Total charge of the compound	-1
Number of carbon atoms	18
Number of heteroatoms	2
Number of heavy atoms	20
Ratio between the number of non-carbon atoms and the number of carbon atoms	0.11
Druggability Properties	
Lipinski's rule of 5 violations	1
Veber rule	Good
Egan rule	Good
Oral PhysChem score (Traffic Lights)	4
GSK's 4/400 score	Good
Pfizer's 3/75 score	Bad
Weighted quantitative estimate of drug-likeness (QEDw) score	0.31
Solubility	2342.23
Solubility Forecast Index	Good
ADMET Properties Property	
Human Intestinal Absorption	HIA+
Blood Brain Barrier	BBB+
Caco-2 permeable	Caco2+
P-glycoprotein substrate	Non-substrate
P-glycoprotein inhibitor I	Non-inhibitor
P-glycoprotein inhibitor II	Non-inhibitor
CYP450 2C9 substrate	Non-substrate
CYP450 2D6 substrate	Non-substrate
CYP450 3A4 substrate	Non-substrate
CYP450 1A2 inhibitor	Inhibitor

CYP450 2C9 inhibitor	Non-inhibitor	0.880
CYP450 2D6 inhibitor	Non-inhibitor	0.963
CYP450 2C19 inhibitor	Non-inhibitor	0.964
CYP450 3A4 inhibitor	Non-inhibitor	0.947
CYP450 inhibitory promiscuity	Low CYP Inhibitory Promiscuity	0.943
Ames test	Non AMES toxic	0.913
Carcinogenicity	Non-carcinogens	0.650
Biodegradation	Ready biodegradable	0.781
Rat acute toxicity	1.328 LD50, mol/kg	NA
hERG inhibition (predictor I)	Weak inhibitor	0.882
hERG inhibition (predictor II)	Non-inhibitor	0.932

Table 3: *In silico* Drug likeliness, Biomolecular Properties and Bioactivity of ALA

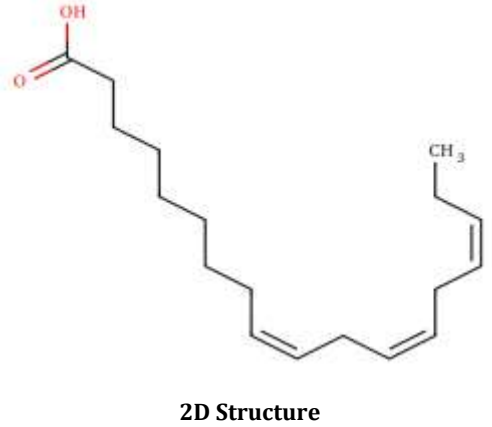
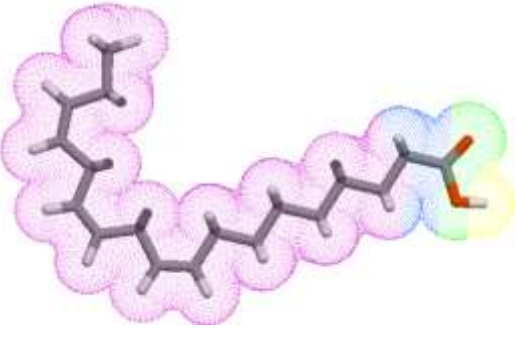
 2D Structure	Molecular Properties	Calculated Values
	miLogP	5.84
	TPSA	37.30
	Natoms	20
	MW	278.44
	nON	2
	nOHNH	1
	Nviolations	1
	Nrotb	13
	volume	306.47
 3D Structure	Biological Properties	Bioactivity Scores
	GPCR ligand	0.33
	Ion channel modulator	0.23
	Kinase inhibitor	-0.19
	Nuclear receptor ligand	0.35
	Protease inhibitor	0.13
	Enzyme inhibitor	0.42

Table 4: Performance measures of vNN models in 10-fold cross validation using a restricted or unrestricted applicability domain

Model	Data ^a	d ₀ ^b	h ^c	Accuracy	Sensitivity	Specificity	kappa	R ^d	Coverage
DILI	1427	0.60	0.50	0.71	0.70	0.73	0.42		0.66
		1.00	0.20	0.67	0.62	0.72	0.34		1.00
Cytotox (Hep2G)	6097	0.40	0.20	0.84	0.88	0.76	0.64		0.89
		1.00	0.20	0.84	0.73	0.89	0.62		1.00
HLM	3219	0.40	0.20	0.81	0.72	0.87	0.59		0.91
		1.00	0.20	0.81	0.70	0.87	0.57		1.00
CYP1A2	7558	0.50	0.20	0.90	0.70	0.95	0.66		0.75
		1.00	0.20	0.89	0.61	0.95	0.60		1.00
CYP2C9	8072	0.50	0.20	0.91	0.55	0.96	0.54		0.76
		1.00	0.20	0.90	0.44	0.96	0.46		1.00
CYP2C19	8155	0.55	0.20	0.87	0.64	0.93	0.58		0.76
		1.00	0.20	0.86	0.52	0.94	0.50		1.00
CYP2D6	7805	0.50	0.20	0.89	0.61	0.94	0.57		0.75
		1.00	0.20	0.88	0.52	0.95	0.51		1.00
CYP3A4	10373	0.50	0.20	0.88	0.76	0.92	0.68		0.78
		1.00	0.20	0.88	0.69	0.93	0.64		1.00
BBB	353	0.60	0.20	0.90	0.94	0.86	0.80		0.61
		1.00	0.10	0.82	0.88	0.75	0.64		1.00
Pgp Substrate	822	0.60	0.20	0.79	0.80	0.79	0.58		0.66
		1.00	0.20	0.73	0.73	0.74	0.47		1.00
Pgp Inhibitor	2304	0.50	0.20	0.85	0.91	0.73	0.66		0.76
		1.00	0.10	0.81	0.86	0.74	0.61		1.00
hERG	685	0.70	0.70	0.84	0.84	0.83	0.68		0.80
		1.00	0.20	0.82	0.82	0.83	0.64		1.00
MMP	6261	0.50	0.40	0.89	0.64	0.94	0.61		0.69
		1.00	0.20	0.87	0.52	0.94	0.50		1.00
AMES	6512	0.50	0.40	0.82	0.86	0.75	0.62		0.79
		1.00	0.20	0.79	0.82	0.75	0.57		1.00
MRTD^e	1184	0.60	0.20					0.79	0.69
		1.00	0.20					0.74	1.00

Table 5: Predicted Targets/ Target Class, Common Name and Probability of LA

TARGET	TARGET CLASS	COMMON.NAME	UNIPROT.ID	PROBABILITY*
Cyclooxygenase-1	Oxidoreductase	PTGS1	P23219	0.858940178705
Peroxisome proliferator-activated receptor gamma	Nuclear receptor	PPARG	P37231	0.554904781379
Peroxisome proliferator-activated receptor alpha	Nuclear receptor	PPARA	Q07869	0.554904781379
Fatty acid binding protein muscle	Fatty acid BPF	FABP3	P05413	0.537563862121
Free fatty acid receptor 1	Family A GPCR	FFAR1	O14842	0.519923086957
Fatty acid binding protein adipocyte	Fatty acid BPF	FABP4	P15090	0.519923086957
Peroxisome proliferator-activated receptor delta	Nuclear receptor	PPARD	Q03181	0.519923086957
Fatty acid binding protein epidermal	Fatty acid BPF	FABP5	Q01469	0.181786517225
Anandamide amidohydrolase	Enzyme	FAAH	O00519	0.164442067635
Telomerase reverse transcriptase	Enzyme	TERT	O14746	0.147106563998
Fatty acid-binding protein, liver	Fatty acid BPF	FABP1	P07148	0.112450964818
Cannabinoid receptor 1	Family A GPCR	CNR1	P21554	0.103761755413
Acyl-CoA desaturase	Enzyme	SCD	O00767	0.0951255886644
Protein-tyrosine phosphatase 1B	Phosphatase	PTPN1	P18031	0.0951255886644
DNA polymerase beta	Enzyme	POLB	P06746	0.0951255886644
Arachidonate 5-lipoxygenase	Oxidoreductase	ALOX5	P09917	0.0951255886644
T-cell protein-tyrosine phosphatase	Phosphatase	PTPN2	P17706	0.0951255886644
Prostaglandin E synthase	Enzyme	PTGES	O14684	0.0951255886644
Leukotriene B4 receptor 1	Family A GPCR	LTB4R	Q15722	0.0951255886644
Carboxylesterase 2	Enzyme	CES2	O00748	0.0951255886644
Estrogen receptor beta	Nuclear receptor	ESR2	Q92731	0.0864426933852
Protein-tyrosine phosphatase 1C	Phosphatase	PTPN6	P29350	0.0864426933852
Protein farnesyltransferase	Enzyme	FNTA FNTB	P49354	0.0864426933852
Nuclear receptor ROR-gamma	Nuclear receptor	RORC	P51449	0.0777583259988
Arachidonate 12-lipoxygenase	Enzyme	ALOX12	P18054	0.0777583259988
11-beta-hydroxysteroid dehydrogenase 1	Enzyme	HSD11B1	P28845	0.0777583259988
DNA topoisomerase I	Isomerase	TOP1	P11387	0.0777583259988
Prostanoid IP receptor	Family A GPCR	PTGIR	P43119	0.0777583259988
Phosphodiesterase 4D	Phosphodiesterase	PDE4D	Q08499	0.0690974435253
Nitric oxide synthase, inducible	Enzyme	NOS2	P35228	0.0690974435253
Prostanoid EP2 receptor (by homology)	Family A GPCR	PTGER2	P43116	0.0690974435253
Dual specificity phosphatase Cdc25A	Phosphatase	CDC25A	P30304	0.0690974435253
Cytochrome P450 19A1	Cytochrome P450	CYP19A1	P11511	0.0604245879294
Glucocorticoid receptor	Nuclear receptor	NR3C1	P04150	0.0604245879294
Vanilloid receptor	Voltage-gated ion chanl	TRPV1	Q8NER1	0.0604245879294
CD81 antigen	Surface antigen	CD81	P60033	0.0604245879294
Protein kinase C eta	Kinase	PRKCH	P24723	0.0604245879294
Receptor- tyrosine-protein phosphatase F	Membrane receptor	PTPRF	P10586	0.0604245879294
LXR-alpha	Nuclear receptor	NR1H3	Q13133	0.0604245879294
Corticosteroid binding globulin	Secreted protein	SERPINA6	P08185	0.0604245879294

Testis-specific androgen-binding protein	Secreted protein	SHBG	P04278	0.0604245879294
Glucose-6-phosphate 1-dehydrogenase	Enzyme	G6PD	P11413	0.0604245879294
Cytochrome P450 51 (by homology)	Cytochrome P450	CYP51A1	Q16850	0.0604245879294
G protein-coupled receptor 44	Family A GPCR	PTGDR2	Q9Y5Y4	0.0604245879294
Protein-tyrosine phosphatase 2C	Phosphatase	PTPN11	Q06124	0.0604245879294
Low molecular weight phosphotyrosine protein	Phosphatase	ACP1	P24666	0.0604245879294
Phospholipase A2 group 1B	Enzyme	PLA2G1B	P04054	0.0604245879294
Steroid 5-alpha-reductase 2	Oxidoreductase	SRD5A2	P31213	0.0604245879294
Prostanoid EP1 receptor	Family A GPCR	PTGER1	P34995	0.0604245879294
Estrogen receptor alpha	Nuclear receptor	ESR1	P03372	0.0604245879294
G-protein coupled receptor 120	Family A GPCR	FFAR4	Q5NUL3	0.0604245879294
HMG-CoA reductase	Oxidoreductase	HMGCR	P04035	0.0604245879294
Niemann-Pick C1-like protein 1	Other membrane protein	NPC1L1	Q9UHC9	0.0604245879294
Sigma opioid receptor	Membrane receptor	SIGMAR1	Q99720	0.0604245879294
Cytochrome P450 17A1	Cytochrome P450	CYP17A1	P05093	0.0604245879294
Prostanoid EP4 receptor	Family A GPCR	PTGER4	P35408	0.0604245879294
Dual specificity phosphatase Cdc25B	Phosphatase	CDC25B	P30305	0.0604245879294
Monocarboxylate transporter 1 (by homology)	Electrochem transporter	SLC16A1	P53985	0.0604245879294
Interleukin-6	Secreted protein	IL6	P05231	0.0604245879294
Glutamine synthetase	Ligase	GLUL	P15104	0.0604245879294
11-beta-hydroxysteroid dehydrogenase 2	Enzyme	HSD11B2	P80365	0.0604245879294
Mineralocorticoid receptor	Nuclear receptor	NR3C2	P08235	0.0604245879294
Adenosine A3 receptor	Family A GPCR	ADORA3	P0DMS8	0.0604245879294
Cyclooxygenase-2	Oxidoreductase	PTGS2	P35354	0.0604245879294
G-protein coupled bile acid receptor 1	Family A GPCR	GPBAR1	Q8TDU6	0.0604245879294
Androgen Receptor	Nuclear receptor	AR	P10275	0.0604245879294
MAP kinase ERK1	Kinase	MAPK3	P27361	0.0604245879294
Progesterone receptor	Nuclear receptor	PGR	P06401	0.0604245879294
Prolyl endopeptidase	Protease	PREP	P48147	0.0604245879294
Autotaxin	Enzyme	ENPP2	Q13822	0.0604245879294
Endothelin receptor ET-A (by homology)	Family A GPCR	EDNRA	P25101	0.0604245879294
Matrix metalloproteinase 13	Protease	MMP13	P45452	0.0604245879294
Matrix metalloproteinase 3	Protease	MMP3	P08254	0.0604245879294
Matrix metalloproteinase 8	Protease	MMP8	P22894	0.0604245879294
Butyrylcholinesterase	Hydrolase	BCHE	P06276	0.0604245879294
Cytosolic phospholipase A2	Enzyme	PLA2G4A	P47712	0.0604245879294
Cytochrome P450 26B1	Cytochrome P450	CYP26B1	Q9NR63	0.0604245879294
Cytochrome P450 26A1	Cytochrome P450	CYP26A1	Q43174	0.0604245879294